0022-3565/09/3301-125–134$20.00
THE JOURNAL OF PHARMACOLOGY AND EXPERIMENTAL THERAPEUTICS
JPET 330:125–134, 2009

Vol. 330, No. 1
151233/3484162
Printed in U.S.A.

Differential Modulation of Farnesoid X Receptor Signaling Pathway by the Thiazolidinediones

Rajani Kaimal, Xiulong Song, Bingfang Yan, Roberta King, and Ruitang Deng

Department of Biomedical and Pharmaceutical Sciences, Center for Pharmacogenomics and Molecular Therapy, College of Pharmacy, University of Rhode Island, Kingston, Rhode Island

Received January 21, 2009; accepted April 13, 2009

ABSTRACT

Thiazolidinediones (TZD), including troglitazone, rosiglitazone, and pioglitazone, are agonists of peroxisome proliferator-activated receptor (PPAR)-γ and belong to a class of insulin-sensitizing drugs for type 2 diabetes mellitus. However, member-specific, PPARγ-independent activities and toxicity have been reported, especially for troglitazone. Currently, the underlying mechanisms are not fully understood. In this study, we demonstrated that troglitazone but not rosiglitazone or pioglitazone modulated expression of farnesoid X receptor (FXR) target genes bile salt export pump (BSEP) and small heterodimer partner (SHP) in Huh-7 cells. More specifically, troglitazone acted as a partial agonist of FXR to weakly increase BSEP and SHP expression but functioned as a potent antagonist to significantly suppress bile acid-induced expression. Consistent with the finding, troglitazone partially induced but markedly antagonized bile acid-mediated BSEP promoter transactivation. However, such modulating effects were not detected with rosiglitazone or pioglitazone. Using the crystal structure of ligand-bound FXR ligand binding domain (LBD), molecular docking predicted that troglitazone, but not rosiglitazone or pioglitazone, could form a stable complex with FXR LBD. The specific α-tocopherol side chain of troglitazone significantly contributed to the formation of such a stable complex through extensive interactions with FXR LBD. The docking model was further validated by functional analyses of a series of docking-guided FXR mutants. In summary, the data demonstrated that troglitazone, but not rosiglitazone or pioglitazone, was an FXR modulator and potently antagonized bile acid-induced expression of FXR target genes. Such differential modulation of FXR signaling pathway by TZDs may represent one of the mechanisms for member-specific, PPARγ-independent activities and toxicity.

Thiazolidinediones (TZD), including troglitazone, rosiglitazone, and pioglitazone, are a class of insulin-sensitizing drugs to treat type 2 diabetes mellitus. Such therapeutic effect of TZDs is achieved through activating nuclear receptor peroxisome proliferator-activated receptor (PPAR)-γ, which is directly involved in the regulation of genes controlling glucose homeostasis and lipid metabolism. Studies also show that TZDs exhibit other important activities, such as cardiovascular, hypertension, and anticancer effects in a PPARγ-dependent or -independent manner (Blanquicett et al., 2008; Rizos et al., 2008).

TZDs are similar in their effects on controlling blood glucose both as monotherapy and in combination therapies. However, member-specific activities and toxicity have been extensively documented, especially for troglitazone. Most notably, severe hepatotoxicity was clinically associated with use of troglitazone, but such association was not observed in patients taking rosiglitazone or pioglitazone (Lebovitz, 2002; Marcy et al., 2004). Troglitazone also exhibited specific activities in inhibiting cell proliferations, including prostate and bladder carcinoma (Chaffer et al., 2006), breast cancer (Lecomte et al., 2008), and hepatoma cells (Bae et al., 2003). Troglitazone also shows unique vasodilating activity (Walker et al., 1998) and distinctively modulates the expression of a diverse array of genes, including cytochrome P450 (Ogino et al., 2002), ATP-binding cassette transporter A1 (Akiyama et

This work was supported in part by the National Institutes of Health National Center for Research Resources [Grant P20-RR016457] (the Rhode Island-Institutional Development Awards Network of Biomedical Research Excellence grant); and by the Rhode Island Foundation [Medical Research Grant 20052653]. B.Y. is supported by the National Institutes of Health [Grants R01GM61988, R01ES07965].

Article, publication date, and citation information can be found at http://jpet.aspetjournals.org.

doi:10.1124/jpet.109.151233.

ABBREVIATIONS: TZD, thiazolidinedione; PPAR, peroxisome proliferator-activated receptor; LBD, ligand binding domain; FXR, farnesoid X receptor; CYP7A1, cholesterol 7α-hydroxylase; BSEP, bile salt export pump; SHP, small heterodimer partner; CDCA, chenodeoxycholic acid; DMSO, dimethyl sulfoxide; DMEM, Dulbecco's modified Eagle's medium; kb, kilobase(s); FXRE, farnesoid X receptor responsive element; IR1, inverted repeat with one nucleotide spacing; PPRE, peroxisome proliferator-activated receptor-responsive element; PCR, polymerase chain reaction; wt, wild type; mut, mutant; Luc, luciferase; GW4064, 3-(2,6-dichlorophenyl)-4-(3′-carboxy-2-chloro-stilben-4-yl)-oxymethyl-5-isopropyl-isoxazole.

al., 2002), phosphoenolpyruvate carboxykinase (Davies et al., 2001), PPARγ (Davies et al., 2002), and insulin-like growth factor binding protein-1 (Hilding et al., 2003). Although considerable efforts have been made to determine the underlying mechanisms for these troglitazone-specific, PPARγ-independent activities and toxicity, our understanding remains largely incomplete.

All of the TZD drugs share a common thiazolidine-2,4-dione core structure, which plays a determinant role in binding to the ligand binding domain (LBD) of PPARγ (Nolte et al., 1998). The side chains of the TZDs differ from each other. Troglitazone has an α-tocopherol, whereas rosiglitazone has an aminopyridyl side chain. It is generally believed that member-specific activities and toxicity are the consequence of differing chemical structures in the side chains of the TZDs.

As a bile acid sensor, nuclear receptor farnesoid X receptor (FXR) is the master regulator for bile acid homeostasis. Bile acid synthesis in liver is initiated by the rate-limiting enzyme cholesterol 7α-hydroxylase (CYP7A1), whereas bile salt export pump (BSEP) is responsible for canalicular secretion of bile acids. Activation of FXR by bile acids directly induces BSEP (Ananthanarayanan et al., 2001) but indirectly represses CYP7A1 expression through induction of small heterodimer partner (SHP), a potent repressor of CYP7A1 transcription (Goodwin et al., 2000). Such coordinate feedback and feed-forward regulation of CYP7A1 and BSEP by bile acids represents an excellent mechanism for preventing excessive accumulation of toxic bile acids in hepatocytes. Indeed, in human, defects in expression or function of BSEP or FXR have been associated with intrahepatic cholestatic liver injury (Wang et al., 2002; Van Mil et al., 2007). In mouse, knockout of FXR, BSEP, or SHP leads to FXR(−/−), BSEP(−/−), or SHP(−/−) mice supersensitive to bile acid- or common bile duct ligation-induced liver toxicity (Sinal et al., 2000; Wang et al., 2001; Park et al., 2008).

In addition to its critical role in maintaining bile acid homeostasis, FXR is also involved in regulating cholesterol, lipid, and glucose metabolism (Wang et al., 2008) and vasculature (Bishop-Bailey et al., 2004). Recent studies have extended its functions into various other nonmetabolic areas, including liver regeneration (Huang et al., 2006) and tumorigenesis (Yang et al., 2007; Modica et al., 2008). Thus, it becomes clear that FXR has much broader activities than what was originally thought.

In this study, we investigated the effects of TZDs on FXR signaling pathway and found that troglitazone, but not rosiglitazone or pioglitazone, was an FXR modulator and potently antagonized bile acid-mediated activation of FXR. Such differential modulation of FXR signaling pathway by TZDs may represent one of the mechanisms for many member-specific, PPARγ-independent activities and toxicity, especially for troglitazone.

Materials and Methods

Chemicals and Supplies. Chenodeoxycholic acid (CDCA), troglitazone, and dimethyl sulfoxide (DMSO) were purchased from Sigma-Aldrich (St. Louis, MO). Rosiglitazone and pioglitazone were from Fisher Scientific (Suwanee, GA). Dulbecco's modified Eagle's medium (DMEM), nonessential amino acids, penicillin-streptomycin solution, Lipofectamine, and Plus reagents were from Invitrogen (Carlsbad, CA). Kits for luciferase detection and the null *Renilla* luciferase plasmid were from Promega (Madison, WI). Fetal bovine sera were from HyClone Laboratories (Logan, UT). Unless otherwise specified, all other reagents were purchased from Fisher Scientific. Oligonucleotides for site-directed mutagenesis were chemically synthesized by Invitrogen.

Plasmid Constructs. Human BSEP promoter reporter pBSEP(−2.6 kb) was constructed by cloning a genomic DNA fragment (2.6 kb) upstream the transcription start site of BSEP into a luciferase reporter vector pGL4.10 (Promega) as described previously (Deng et al., 2006). Human BSEP promoter reporter mutant pBSEP-IR1-mut carrying mutations in the FXR-responsive element (FXRE), an inverted repeat with one nucleotide spacing (IR1), was made as described previously (Deng et al., 2006). Construct of the PPAR-responsive element (PPRE) reporter, pPPRE-Luc, containing four copies of the PPRE derived from rat acyl-CoA oxidase, was kindly provided by Dr. Matthew Stoner (University of Rhode Island, Kingston, RI) (Stoner et al., 2007). The FXRE-containing reporter derived from phospholipid transfer protein pTK-FXRE-Luc was kindly provided by Dr. Peter Edwards (UCLA, Los Angeles, CA). Expression plasmids for human nuclear receptors FXR and PPARγ were kindly provided by Dr. David Mangelsdorf (University of Texas Southwestern Medical Center, Dallas, TX) and Dr. Te-Jin Chow (Fooyin University, Taipei City, Taiwan), respectively.

Hepatoma Cell Culture and Treatments. Hepatoma Huh-7 cells purchased from American Type Culture Collection (Manassas, VA) were maintained in DMEM containing 10% fetal bovine serum, 1% penicillin/streptomycin, and 1× nonessential amino acids. Cells were seeded at a density of 2×10^5 cells/well (12-well plates). Sixteen hours after seeding, cells were treated with vehicle DMSO (0.1%, v/v), troglitazone (10 μM), rosiglitazone (10 μM), pioglitazone (10 μM), CDCA (5 μM), or a combination of CDCA and troglitazone, rosiglitazone, or pioglitazone for 48 h.

Reverse Transcription-Coupled Real-Time Polymerase Chain Reaction. Total RNA was isolated from treated cells as described previously (Deng et al., 2006) and was subjected to synthesis of the first-strand cDNA with random primers and ThermoScript I reverse transcriptase (Invitrogen). The reactions were incubated initially at 25°C for 10 min and then at 50°C for 50 min, followed by inactivation of the reaction at 70°C for 10 min. The cDNAs were then diluted eight times with water and subjected to real-time PCR using TaqMan Gene Expression Assay (Applied Biosystems, Foster City, CA) (Deng et al., 2007). The TaqMan assay mixtures for human BSEP (assay ID: Hs00184824_m1), SHP (assay ID: Hs00222677_m1), and glyceraldehydes-3-phosphate dehydrogenase (assay ID: 4352934E) were purchased from Applied Biosystems. The real-time PCR was performed using TaqMan Universal PCR Master Mix (Applied Biosystems), following the instructions of the manufacturer, in a total volume of 20 μl containing 9 μl of universal PCR master mix, 1 μl of gene-specific TaqMan assay mixture, and 6 μl of cDNA templates. Cycling profile was as follows: 50°C for 2 min, 95°C for 10 min, followed by 40 cycles of 15 s at 95°C and 1 min at 60°C, as recommended by the manufacturer. Amplification and quantification were done with a 7500 Real-Time PCR System (Applied Biosystems).

Reporter Luciferase Assay. Huh-7 cells were plated in 24-well plates in DMEM supplemented with 10% fetal bovine serum at a density of 8×10^4 cells per well and cultured overnight. Transient transfection was conducted by lipofection with Lipofectamine and Plus reagent (Invitrogen) as described previously (Deng et al., 2006). For all of the transfections, standard amounts of plasmid DNA used per well were 100 ng for promoter construct, 100 ng for nuclear receptor expression plasmids, and 10 ng for the null *Renilla* luciferase plasmid as an internal control. After cells were transfected for 3 h, 0.5 ml of fresh medium was added into each well, and cells were incubated overnight. The next day, cell supernatants were replaced with treatment medium containing appropriate chemicals at a concentration specified in the figure legends. The treatment was continued for 30 h unless specified otherwise. The luciferase activities were assayed with a Dual-Luciferase Reporter Assay System as

described previously (Deng et al., 2006). In brief, treated Huh-7 cells were washed once with phosphate-buffered saline and lysed by adding 100 μl of passive lysis buffer with gentle rocking for 30 min. Ten microliters of cell lysates was transferred to a 96-well reader plate, and luciferase activities were measured by a Berthold Technologies microplate luminometer (PerkinElmer Life and Analytical Sciences, Boston, MA). The firefly luminescence was normalized based on the *Renilla* luminescence signal, and the ratio of treatment over control served as -fold activation. Data are presented as mean ± S.D. of at least three separate experiments.

Molecular Docking. To better understand the interaction of troglitazone with FXR, molecular docking with Autodock 4.1(The Scripps Research Institute, La Jolla, CA) was performed. The objective was to find the best ligand conformer with the least binding energy and to identify the amino acids critical for the interaction. CDCA, a natural ligand of FXR, along with rosiglitazone and pioglitazone were included in the docking study as positive and negative controls, respectively.

The crystal structure of human FXR LBD (Protein Data Bank identification code 1OSH) (Downes et al., 2003) was used as receptor template. The docking cavity of crystal ligand fexaramine served as the initial pocket or grid box for docking of all the ligands. Three dimensional structures of the four compounds were built and optimized using ChemDraw Ultra 11 (CambridgeSoft Corporation, Cambridge, MA). Each compound was then individually docked to FXR LBD using Autodock 4.1 (Morris et al., 1998). By default, the program adds Gasteiger charges and computes the torsions for each compound. The torsions for CDCA, troglitazone, rosiglitazone, and pioglitazone were set at 7, 6, 7, and 7, respectively. The initial dockings for each compound were carried out using the grid box parameters of the crystal ligand and default settings. The dockings were carried out using Lamarckian genetic algorithm (Morris et al., 1998). One hundred genetic algorithms were carried out with a population size of 300. The maximal number of evaluations was set at 25 million and the maximal number of generations was set at 27,000, which is considered ideal for compounds with torsions between 1 and 10. Based on initial docking, the conformer with the least energy for each compound was chosen for subsequent dockings using the grid box parameters of this conformer. Repeated dockings were carried out until no further refinement in clustering or binding energy of conformer was achieved. Based on population size and binding energy, the best docked conformation was chosen for further analysis of protein-ligand interaction (http://ligpro.sdsc.edu/).

Site-Directed Mutagenesis. Mutagenesis was performed using QuikChange site-directed mutagenesis kit (Stratagene, La Jolla, CA) and FXR wt as template (Song et al., 2008). The sequences of the mutagenesis oligonucleotides were listed in Table 1. The mutagenesis reactions were performed essentially as recommended by the manufacturer (Stratagene, La Jolla, CA). The resulting mutants were subjected to sequence analysis to confirm the desired substitutions being made without introducing errors.

Statistic Analysis. Student's *t* test was applied to pairwise comparison to determine the statistic significance. Values of 0.05 or lower were considered significant.

Results

Troglitazone but Not Rosiglitazone or Pioglitazone Modulated BSEP and SHP Expression. Both BSEP and SHP are FXR target genes involved in maintaining bile acid homeostasis in the liver. To determine whether TZD drugs modulate FXR signaling pathway, the effects of the three TZD drugs on BSEP and SHP mRNA levels were investigated in human hepatoma Huh-7 cells with TaqMan real-time PCR. CDCA and DMSO were included in the treatments as positive and negative control, respectively. As shown in Fig. 1, A and B, similar to vehicle DMSO, rosiglitazone or pioglitazone had no detectable effect on BSEP and SHP mRNA expression. However, BSEP and SHP expression was weakly, but statistically significantly, induced in cells treated with troglitazone (approximately 2.5- and 1.8-fold induction for BSEP and SHP, respectively). As expected, CDCA strongly induced BSEP expression by approximately 15-fold and SHP by 3.5-fold. However, such strong induction was significantly suppressed by troglitazone with 59% reduction for BSEP and 56% for SHP. In contrast, minimal suppression was detected in cells treated with rosiglitazone or pioglitazone. It should be noted that certain cell death was observed in wells treated with CDCA and pioglitazone. As a result, relatively larger variations were obtained. Taken together, the data demonstrated that distinct from rosiglitazone and pioglitazone, troglitazone weakly induced BSEP and SHP expression but significantly suppressed their expression induced by bile acid.

To further investigate the suppressing effect of troglitazone on bile acid-induced expression of BSEP and SHP, a dose-response study was performed. As shown in Fig. 1, C and D, troglitazone dose-dependently decreased CDCA-induced expression of BSEP and SHP. Significant decrease (approximately 30% reduction) in BSEP and SHP expression was detected in cells treated with troglitazone at a concentration of 5 μM, and such repression reached to more than 70% at the concentration of 20 μM.

Troglitazone Modulated BSEP Transactivation through FXR Signaling Pathway. The distinct effect of troglitazone from rosiglitazone and pioglitazone on BSEP and SHP expression suggests that PPARγ activation is unlikely the mechanism for troglitazone to modulate BSEP and

TABLE 1
Sequences of mutagenesis oligonucleotides
The mutated nucleotides are underlined.

Oligonucleotide	Sequence (5′–3′)
F288H-sense[a]	AGAATTCAGTGCAGAAGAAAATCATCTCATTTTGACGGAAATGGCAACC
F288H-antisense	GGTTGCCATTTCCGTCAAAATGAGATGATTTTCTTCTGCACTGAATTCT
L291Y-sense	GCAGAAGAAAATTTTCTCATTTATACGGAAATGGCAACCAATCATGTACA
L291Y-antisense	TGTACATGATTGGTTGCCATTTCCGTATAAATGAGAAAATTTTCTTCTGC
T292L-sense	GAAGAAAATTTTCTCATTTTGCTGGAAATGGCAACCAATCATGTACAGGTT
T292L-antisense	AACCTGTACATGATTGGTTGCCATTTCCAGCAAAATGAGAAAATTTTCTTC
A295Y-sense	AAATTTTCTCATTTTGACGGAAATGTACACCAATCATGTACAGGTTCTTG
A295Y-antisense	CAAGAACCTGTACATGATTGGTGTACATTTCCGTCAAAATGAGAAAATTT
M332T-sense	GCTGAAAGGGTCTGCGGTTGAAGCTACGTTCCTTCGTTCAGCTGAGATTTTC
M332T-antisense	GAAAATCTCAGCTGAACGAAGGAACGTAGCTTCAACCGCAGACCCTTTCAGC
L352Y-sense	CTTCCGTCTGGGCATTCTGACCTATATGAAGAAAGAATTCGAAATAGTGGT
L352Y-antisense	ACCACTATTTCGAATTCTTTCTTCATATAGGTCAGAATGCCCAGACGGAAG

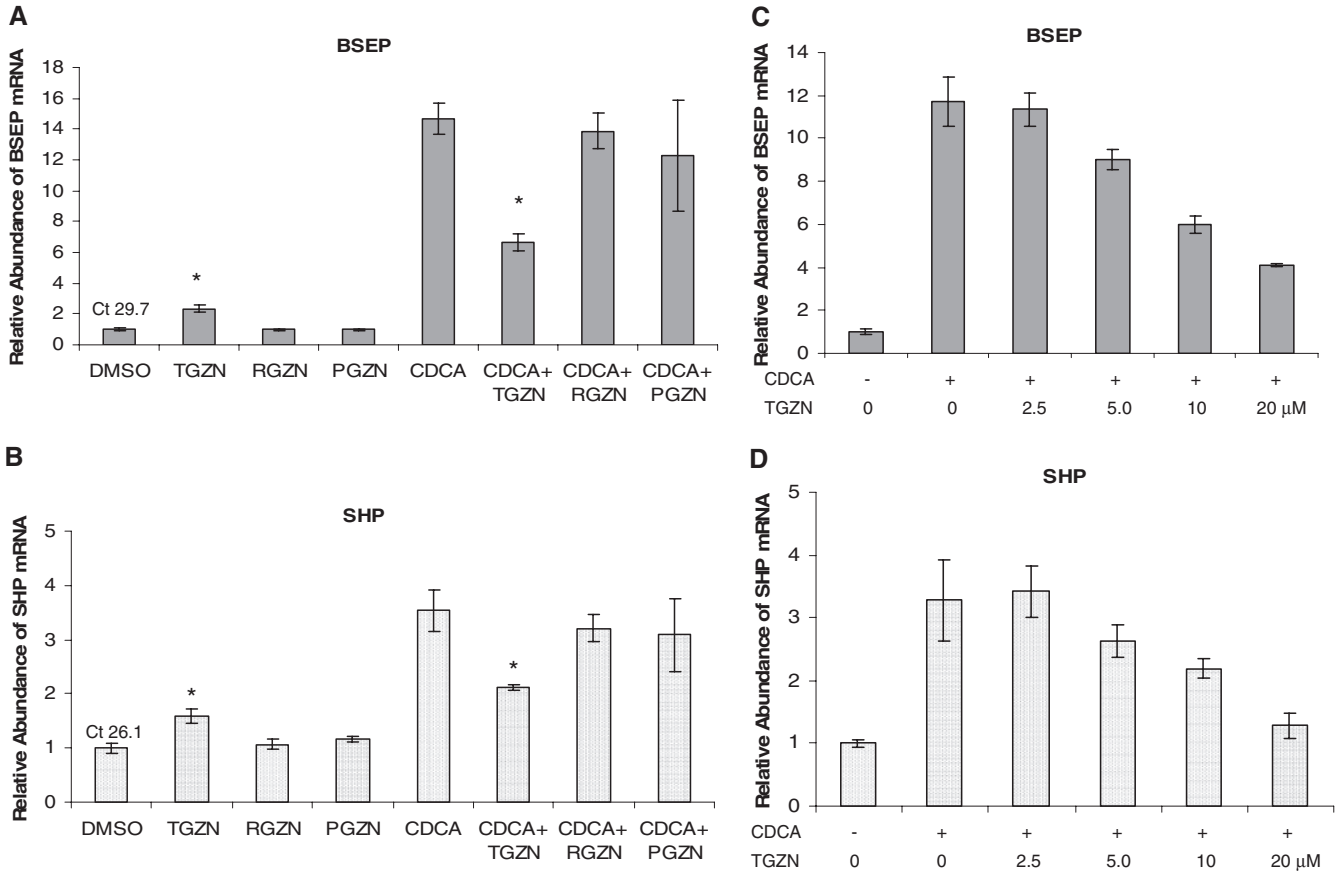

Fig. 1. Troglitazone, but not rosiglitazone or pioglitazone, modulated BSEP and SHP mRNA expression. A, BSEP mRNA abundance: Huh-7 cells seeded in 12-well plates were treated with vehicle DMSO (0.1%), troglitazone (TGZN) (10 μM), rosiglitazone (RGZN) (10 μM), pioglitazone (PGZN) (10 μM), CDCA (5 μM), or CDCA with either troglitazone, rosiglitazone, or pioglitazone for 48 h. Total RNA was isolated and subjected to cDNA synthesis and real-time PCR using TaqMan Gene Expression Assay with BSEP-specific probe. The mRNA levels for glyceraldehydes-3-phosphate dehydrogenase were detected as internal control. The data are presented as mean ± S.D. of at least three separate experiments. Student's *t* test was applied to determine the significance of the differences between DMSO- and troglitazone-treated group or CDCA and CDCA with troglitazone-treated group. The asterisk (∗) indicates a significant difference ($P < 0.05$). The PCR cycle times (Ct) value in cells treated with vehicle DMSO are given on the top of the column. B, SHP mRNA abundance: exactly the same treatments as described above except for using SHP-specific probe. C, dose study for BSEP: Huh-7 cells were treated with vehicle DMSO (0.1%) or CDCA (5 μM) with increasing concentrations of troglitazone (0, 2.5, 5.0, 10, and 20 μM) for 48 h. BSEP mRNA levels were detected by the TaqMan real-time PCR assays. D, dose study for SHP: exactly the same treatments as described in C, except for using SHP-specific probe.

SHP expression. To conclusively exclude such possibility, we investigated the effect of PPARγ activation on BSEP promoter transactivation. As shown in Fig. 2A, as PPARγ agonists, all three drugs markedly induced transactivation of a pPPRE-Luc reporter. At a concentration of 10 μM, rosiglitazone and pioglitazone showed more potent agonistic activities than troglitazone, consistent with the ranking order of the PPARγ binding potencies of the drugs (Willson et al., 1996; Camp et al., 2000). In contrast, all of the three drugs had no effects on BSEP transactivation in the presence of PPARγ, consistent with the notion that BSEP is not a PPARγ target gene and that PPARγ activation is not the mechanism for the effect of troglitazone on BSEP expression.

We next performed experiments to determine whether troglitazone-mediated modulation of BSEP mRNA expression is at the transcriptional level through FXR signaling pathway. The effects of troglitazone on BSEP promoter transactivation in the absence or presence of nuclear receptors FXR were evaluated. As shown in Fig. 2B, in the presence of FXR, the level of basal transactivation of BSEP promoter was increased, consistent with BSEP being an FXR target gene. It is more important to note that such elevated transactivation was further increased by troglitazone by approximately 2.5-fold. In contrast, rosiglitazone and pioglitazone had minimal effects. As expected, CDCA strongly increased BSEP transactivation (approximately 7-fold). The data suggested that troglitazone modulates BSEP expression at the transcriptional level through FXR signaling pathway.

To further confirm such FXR-dependent modulation of BSEP transactivation, the effects of troglitazone on FXR(Y361L) and BSEP promoter mutant (pBSEP-IR1-mut) were determined. Both FXR(Y361L) and pBSEP-IR1-mut totally loss or significantly decrease the ability to respond to FXR ligands (Deng et al., 2006). As shown in Fig. 2B, mutation in FXR or FXRE of BSEP promoter almost abolished the ability of troglitazone to transactivate BSEP. The results thus demonstrated that troglitazone-mediated transactivation of BSEP was FXR- and FXRE-dependent. Taken together, the data demonstrated that troglitazone modulated BSEP transactivation through the FXR signaling pathway.

Troglitazone, but Not Rosiglitazone or Pioglitazone, Antagonized Bile Acid-Mediated Transactivation of BSEP Promoter. We demonstrated previously that troglitazone significantly decreased CDCA-induced BSEP expres-

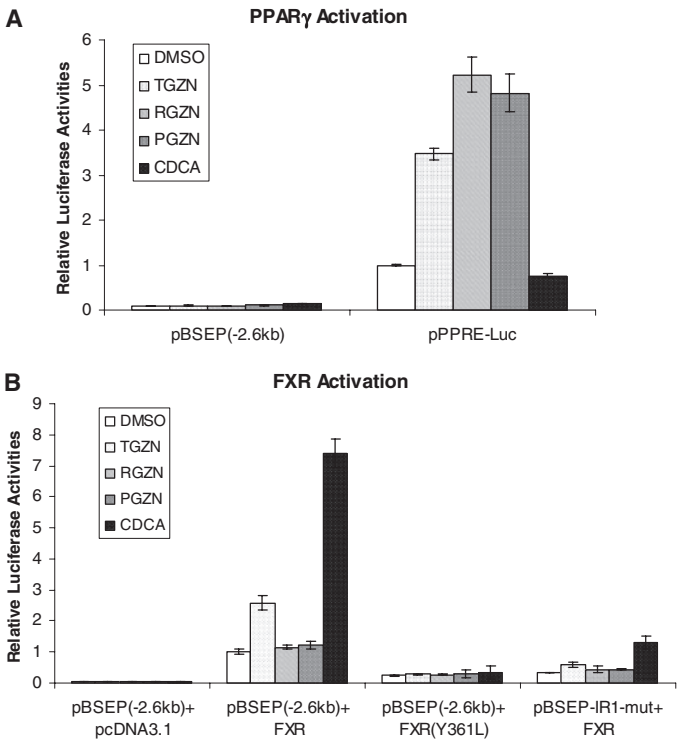

Fig. 2. Troglitazone modulated BSEP transactivation through FXR signaling pathway. A, Huh-7 cells seeded in 24-well plates were transfected with 100 ng of human PPARγ expression plasmid, 10 ng of the null *Renilla* luciferase plasmid as an internal control, and 100 ng of human BSEP promoter reporter pBSEP(−2.6kb) or 100 ng of PPARE-containing reporter pPPRE-Luc. Sixteen hours after transfection, cells were treated with vehicle DMSO (0.1%), troglitazone (TGZN) (10 μM), rosiglitazone (RGZN) (10 μM), pioglitazone (PGZN) (10 μM), and CDCA (10 μM) for 30 h, followed by detection of luciferase activities with a Dual-Luciferase Reporter Assay System. The firefly luminescence was normalized based on the *Renilla* luminescence signal. The data are presented as mean ± S.D. of at least three separate experiments. B, Huh-7 cells were cotransfected with a reporter [pBSEP(−2.6kb) or pBSEP-IR1-mut] (100 ng), FXR expression plasmid [FXR wt, FXR(Y361L) mutant, or pcDNA3.1 empty vector as negative control] (100 ng), and null *Renilla* luciferase plasmid (10 ng) as internal control, followed by treatments of transfected cells and detection of luciferase activities as described in A.

sion (Fig. 1). To determine whether such decrease is mediated through antagonizing CDCA-mediated FXR activation, the effect of troglitazone on CDCA/FXR-mediated transactivation of BSEP promoter was evaluated. As shown in Fig. 3A, CDCA strongly induced BSEP transactivation (approximately 8-fold) in the presence of FXR. However, such strong induction was significantly reduced in cells treated with troglitazone (approximately 70% reduction). In contrast, no significant effects were detected with rosiglitazone or pioglitazone (Fig. 3A). The data thus demonstrated that troglitazone decreased bile acid-induced BSEP expression through antagonizing FXR.

To further investigate the antagonizing effect of troglitazone on BSEP transactivation, a dose-response study was performed. As shown in Fig. 3B, significant decrease in luciferase activity was detected in cells treated with troglitazone at a concentration of 1 μM. Additional reductions were detected in cells treated with higher doses and reached a maximum (approximately 80% decrease) in cells treated with 20 μM troglitazone. Thus, the data showed that troglitazone dose-dependently antagonized CDCA-induced BSEP transactivation. It should be mentioned that troglitazone at concentrations higher than 20 μM caused cell death; thus, the data with higher doses were not reported.

After determining that troglitazone modulates BSEP transactivation through FXR signaling pathway, we then confirmed such finding by demonstrating the similar modulating effects of troglitazone on transactivation of an FXRE reporter, pTK-FXRE-Luc. As shown in Fig. 3C, troglitazone weakly but significantly induced FXRE transactivation (2.3-fold). However, it markedly antagonized CDCA-mediated transactivation (approximately 70% repression). Again, rosiglitazone and pioglitazone exhibited minimal effects.

Troglitazone Could Form Stable Complex with FXR LBD in Molecular Docking. The results obtained with BSEP expression and transactivation indicated that troglitazone was an FXR modulator with potent antagonistic activity. To provide additional evidence to support such notion, the ability of troglitazone to bind to the FXR LBD was evaluated by molecular docking. The chemical structures of CDCA, troglitazone, rosiglitazone, and pioglitazone were given in Fig. 4A. In comparison, it is noted that the side chain of troglitazone, α-tocopherol, is much bigger in size than the side chain of rosiglitazone or pioglitazone.

The crystal structure of human FXR LBD was used as the template and the docking cavity of crystal ligand fexaramine served as the initial pocket for docking of troglitazone. CDCA, rosiglitazone, and pioglitazone were included in the evaluation as positive and negative controls. As shown in Fig. 4B, among potential 100 conformers, a dominant conformer cluster (representing 69% of the conformers) with binding energy of −9.4 kcal/mol was predicted for CDCA, consistent with CDCA being the most potent endogenous FXR agonist. It is more important to note that a dominant conformer cluster (representing 67% of the conformers) with a binding energy of −10.8 kcal/mol was predicted for troglitazone. In contrast, no dominant conformer clusters were identified for rosiglitazone or pioglitazone, even in a higher energy range. The data indicated that similar to CDCA, troglitazone, but not rosiglitazone or pioglitazone, was able to bind to FXR LBD with high affinity.

Based on the initial docking, the least energy conformer for troglitazone and CDCA was chosen for subsequent refinement and used for further analysis of protein-ligand interaction. The predicted models for binding of CDCA and troglitazone to FXR LBD in two different viewing angles are presented in Fig. 5A. Based on the models, CDCA and troglitazone could potentially form hydrogen bond with residue Leu352. Hydrogen bonding was also predicted between residue Leu291 and CDCA but not troglitazone. Both CDCA and troglitazone shared extensive interactions of their main body with residues in α-helix 3, -5, -6, -7, and -11/12 (Fig. 5A). Those residues included Met294, Ala295, Met332, Phe340, Leu352, Ile356, Ile361, Met369, Tyr373, Met454, and Trp473, most of which were involved in hydrophobic interaction. In contrast, residues Tyr365 and Arg355 were predicted to selectively interact with CDCA, whereas residues Phe288, Leu469, Phe465, Thr292, and Trp458 were predicted to uniquely interact with troglitazone (Fig. 5A).

The docking model predicted that the α-tocopherol side chain of troglitazone sit in a position in the ligand binding cavity comparable with the A/B ring of CDCA with a longer

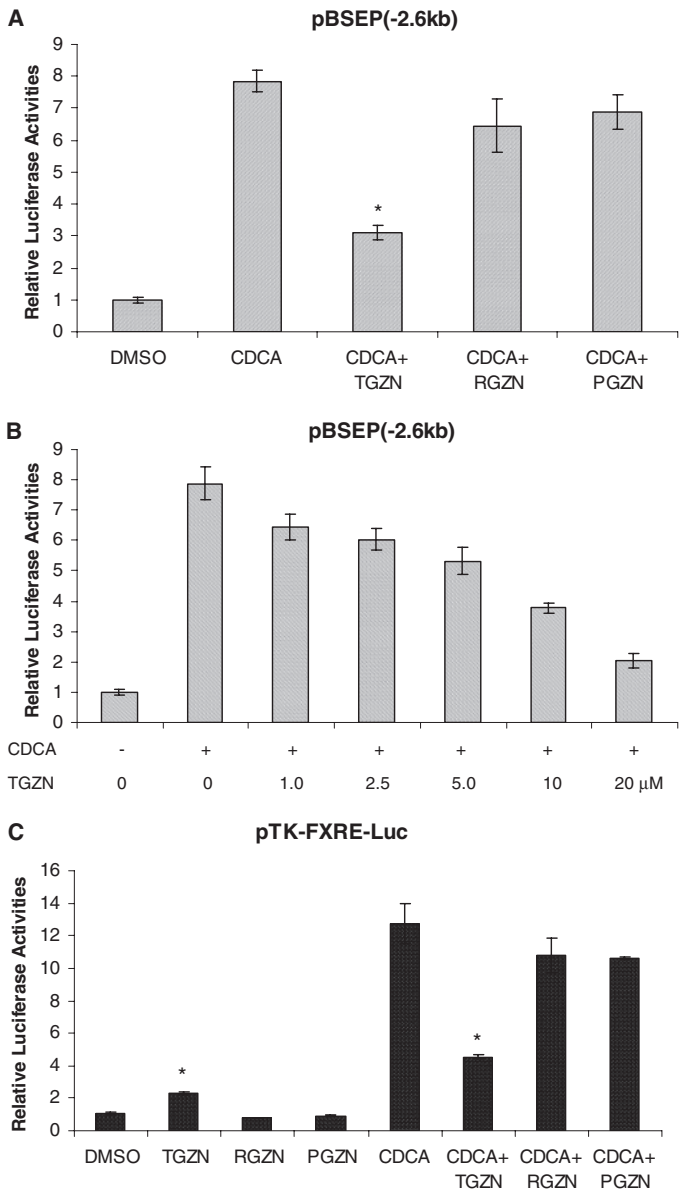

Fig. 3. Troglitazone antagonized CDCA-mediated transactivation of BSEP promoter and FXRE-containing reporter. A, Huh-7 cells seeded in 24-well plates were cotransfected with human BSEP promoter reporter pBSEP(−2.6kb) (100 ng), FXR expression plasmid (100 ng), and null *Renilla* luciferase plasmid (10 ng) as internal control. Sixteen hours after transfection, cells were treated with vehicle DMSO (0.1%), CDCA (10 μM), or CDCA with either troglitazone (TGZN) (10 μM), rosiglitazone (RGZN) (10 μM), or pioglitazone (PGZN) (10 μM) for 30 h, followed by detection of luciferase activities with a Dual-Luciferase Reporter Assay System. The asterisk (*) indicates a significant difference ($P < 0.05$) between CDCA and CDCA + TGZN by Student's t test. B, Huh-7 cells were cotransfected with human BSEP promoter reporter pBSEP(−2.6kb) (100 ng), FXR expression plasmid (100 ng), and null *Renilla* luciferase plasmid (10 ng). Sixteen hours after transfection, cells were treated with vehicle DMSO (0.1%) or CDCA (5 μM) with increasing concentrations of troglitazone (0, 1.0, 2.5, 5.0, 10, and 20 μM) for 30 h, followed by detection of luciferase activities with the Dual-Luciferase Reporter Assay System. C, Huh-7 cells were transfected with FXR expression plasmid (100 ng), FXRE-containing reporter pTK-FXRE-Luc (100 ng), and null *Renilla* luciferase plasmid (10 ng). Sixteen hours after transfection, cells were treated with vehicle DMSO (0.1%), troglitazone (TGZN) (10 μM), rosiglitazone (RGZN) (10 μM), pioglitazone (PGZN) (10 μM), CDCA (5 μM), or CDCA with either troglitazone, rosiglitazone, or pioglitazone for 30 h. Luciferase activity was assayed with a Dual-Luciferase Reporter Assay System. The asterisk (*) indicates a significant difference ($P < 0.05$) between DMSO and TGZN or CDCA and CDCA + TGZN by Student's t test. All the data are presented as mean ± S.D. of at least three separate experiments.

extension (Fig. 5A). Extensive interactions between the α-tocopherol side chain and FXR LBD were predicted. Majority of the residues involved in interaction with the α-tocopherol side chain were located in α-helix 3 and -11/12, including Phe288, Leu291, Thr292, Ala295, Ile361, Trp458, Phe465, Leu469, and Trp473 (Fig. 5B). The results indicated that the α-tocopherol significantly contributed to the stable binding of troglitazone to FXR LBD. With a much smaller side chain than the α-tocopherol, rosiglitazone or pioglitazone presumably could not fully occupy the ligand binding cavity, thus failing to form a stable complex with FXR. Taken together, the docking model predicted that troglitazone but not rosiglitazone or pioglitazone could bind to the LBD of FXR with high affinity and that the α-tocopherol side chain of troglitazone significantly contributed to the binding.

Functional Analysis of Docking-Guided FXR Mutants. To validate the docking models of troglitazone or CDCA with FXR LBD, mutational analysis was carried out. Six amino acid residues in the FXR LBD predicted to participate in the interaction with troglitazone and/or CDCA were selected for the analysis (Fig. 6A). Residues Ala295, Met332, and Leu352 were predicted to interact with both troglitazone and CDCA and mutated to Tyr295, Thr332, and Tyr352, respectively, resulting in FXR mutants FXR(A295Y), FXR(M332T), and FXR(L352Y). Consistent with the prediction, mutation of residues Ala295 and Leu352 to tyrosine completely lost the ability of FXR mutants to respond to both troglitazone and CDCA (Fig. 6B). Substitution of Met332 with threonine completely diminished FXR activation by troglitazone, whereas the mutant partially maintained its ability to respond to CDCA (Fig. 6B). Interestingly, the -fold induction by CDCA was actually increased from 7.7 with FXR wt to 10.8 with FXR(M332T) due to significant decrease in basal activation detected in cells treated with DMSO. Furthermore, although troglitazone failed to activate FXR(M332T), its antagonistic activity against CDCA-mediated transactivation was actually enhanced (Fig. 6A). Approximately 85% reduction in activation was detected in cells treated with CDCA and troglitazone compared with cells treated with CDCA alone, indicating that troglitazone was still able to bind to the mutant and acted as a much stronger antagonist to suppress CDCA-mediated activation of the FXR(M332T) mutant.

Residue Leu291 was predicted to differentially interact with CDCA and troglitazone. It could potentially form hydrogen bond with CDCA, whereas such hydrogen bonding was not predicted for troglitazone. Consistent with the prediction, mutation of Leu291 to tyrosine resulted in complete loss of the ability of FXR to respond to CDCA, whereas its ability to respond to troglitazone remained intact (Fig. 6C). Phe288 and Thr292 were predicted to specifically contact with troglitazone. As predicted, both FXR(F288H) and FXR(T292L) mutants lost their abilities to respond to troglitazone. However, their ability to respond to CDCA was also diminished. The results thus suggested that the two residues played important roles in interacting with both troglitazone and CDCA. Taken together, the data from mutational analyses substantially support the docking models, and the selected residues were critically involved in interacting with troglitazone and/or CDCA.

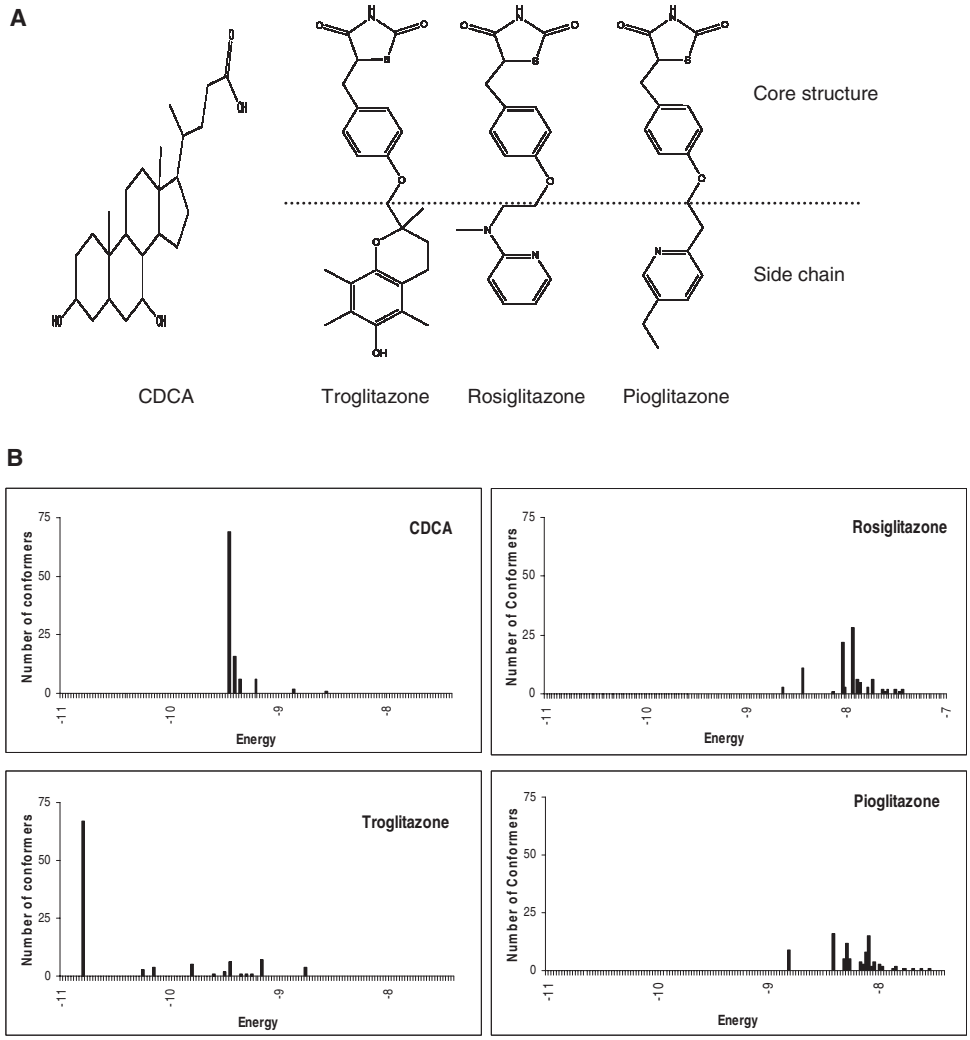

Fig. 4. Troglitazone could form stable complex with FXR LBD in molecular docking. A, the chemical structures of CDCA, troglitazone, rosiglitazone, and pioglitazone. B, the crystal structure of human FXR LBD (Protein Data Bank identification code 1OSH) (Downes et al., 2003) was used as receptor template and the docking cavity of crystal ligand fexaramine served as the initial pocket or grid box for docking of troglitazone, pioglitazone, rosiglitazone, and CDCA. Three-dimensional structures of the four compounds were built and optimized using ChemDraw Ultra 11 (CambridgeSoft Corporation). Each compound was then individually docked to FXR LBD using Autodock 4.1 (Morris et al., 1998). The top 100 conformers with the least binding energy were predicted for each compound.

Discussion

Nuclear receptors, including PPARγ and FXR, are a group of ligand-activated transcription factors regulating expression of genes involved in the synthesis, metabolism, and disposition of steroids, cholesterol, lipids, and bile acids. Nuclear receptors are prime candidates as drug targets. However, development of such drugs faces challenge for their specificity and selectivity. Nuclear receptors not only share transcriptional targets but also many serve as transcriptional inducers of one another. Equally challenging is that ligands are often not selective for one particular target nuclear receptor, but rather are ligands for other receptors. In this study, we demonstrated that as a PPARγ agonist, troglitazone is also an FXR modulator and antagonizes the bile acids/FXR signaling pathway. Thus, distinct from rosiglitazone and pioglitazone, troglitazone acted as a dual ligand for both PPARγ and FXR. Similar overlapping ligand specificity phenomenon has also been reported for a class of polyunsaturated fatty acids, including arachidonic acid, docosahexaenoic acid, and linolenic acid (Zhao et al., 2004). Those polyunsaturated fatty acids are endogenous agonists of PPAR, antagonists of nuclear receptor liver X receptor, and ligands of FXR differentially modulating FXR target gene expression. The complex intertwining network regulated by those closely related nuclear receptors with overlapping ligand specificity imposes the challenge for development of receptor-specific drugs. Off-target activation or antagonism of other nuclear receptors produces unexpected pharmacological effects and/or imposes a great risk for drug safety. Global gene profiling may provide a solution for meeting such challenge.

As a bile acid sensor, nuclear receptor FXR is the master regulator for bile acid homeostasis. Activation of FXR by bile acids directly leads to up-regulation of BSEP and indirectly to down-regulation of CYP7A1 through inducing SHP expression, resulting in increased bile acid secretion and decreased bile acid synthesis in the liver (Goodwin et al., 2000; Ananthanarayanan et al., 2001). Such coordinated positive and negative regulation of BSEP and CYP7A1, respectively, by FXR activation is a protective mechanism for preventing excessive accumulation of toxic bile acids in the liver. In this study, we demonstrated that as an FXR modulator, troglitazone antagonized the bile acid/FXR signaling pathway and significantly repressed bile acid-induced BSEP and SHP expression. Repression of BSEP and SHP expression by troglitazone presumably leads to a decrease in bile acid secretion and an increase in bile acid synthesis, respectively. Such compounding effects potentially cause excessive hepatic accumulation of bile acids, causing hepatotoxicity. Therefore, troglitazone-mediated antagonism of FXR may represent one of the mechanisms for troglitazone-specific, PPARγ-indepen-

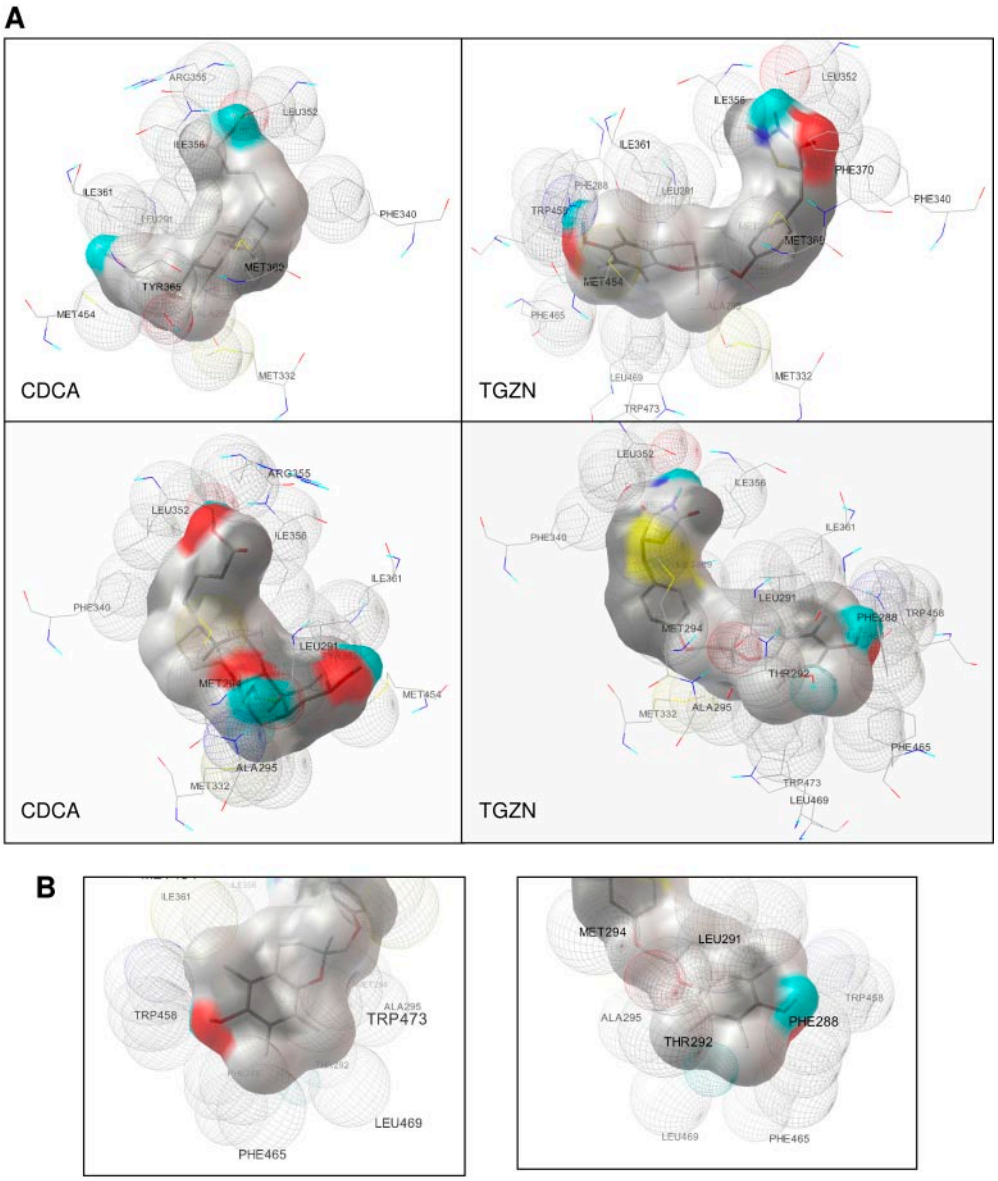

Fig. 5. Docking models of troglitazone and CDCA with FXR LBD. A, based on initial docking, the conformer the least energy for troglitazone or CDCA was chosen for subsequent dockings using the grid box parameters of this conformer. Repeated dockings were carried out until no further refinement in clustering or binding energy of conformer was achieved. Based on population size and binding energy, the best docked conformation was chosen for further analysis of protein-ligand interaction. The docking models with two different viewing angles were presented for both CDCA and troglitazone (TGZN). The amino acid residues predicted to interact with the ligands are shown. B, predicted interaction between the α-tocopherol side chain of troglitazone and amino acid residues of FXR LBD are presented in two different viewing angles.

dent hepatotoxicity. Consistent with this speculation are the findings that antagonizing FXR activation is a mechanism for lithocholic acid-induced liver toxicity (Yu et al., 2002), whereas synthetic FXR agonist GW4064 prevents intra- and extrahepatic cholestatic injury (Liu et al., 2003).

Troglitazone exhibited anticancer activities by either inhibiting cell proliferation or promoting apoptosis. Studies have shown that troglitazone induced G_1 arrest and apoptosis of hepatoma cells, but such effects are not observed with rosiglitazone (Bae et al., 2003). Troglitazone also inhibits proliferation and growth of colon cancer (Ming et al., 2006), prostate carcinoma (Chaffer et al., 2006), and estrogen receptor-α-dependent breast cancer cells (Lecomte et al., 2008). The mechanisms for those PPARγ-independent anticancer activities of troglitazone are largely unknown. In this study, we demonstrated that troglitazone was an FXR modulator. Recent studies have established that FXR plays a protective role in carcinogenesis in the liver and intestine. Such protective function is convincingly demonstrated by the findings that FXR deficiency in mouse causes spontaneous hepatocarcinoma (Yang et al., 2007) and increases intestinal epithelial cell proliferation and tumor development (Modica et al., 2008). It has also been reported that FXR is expressed in normal and cancer prostate epithelial cells and plays a role in cell proliferation by regulating androgen metabolism (Kaeding et al., 2008). In breast cancer cells, FXR activation has been associated with either induction of cell apoptosis (Swales et al., 2006) or promotion of breast cancer cell growth (Journe et al., 2008). Thus, it seems that both FXR and troglitazone play a role in those types of cancers. Modulation of FXR signaling pathway may be related to those anticancer activities of troglitazone; however, further studies are required to support such speculation.

The different pharmacological and clinical safety profiles among those TZD drugs suggest that the side chains rather than the core structure of the drugs play a critical role in determining the member-specific, PPARγ-independent activities. Indeed, the α-tocopherol side chain of troglitazone was predicted by the molecular docking to participate in extensive interactions with FXR LBD (Fig. 5, A and B). In contrast,

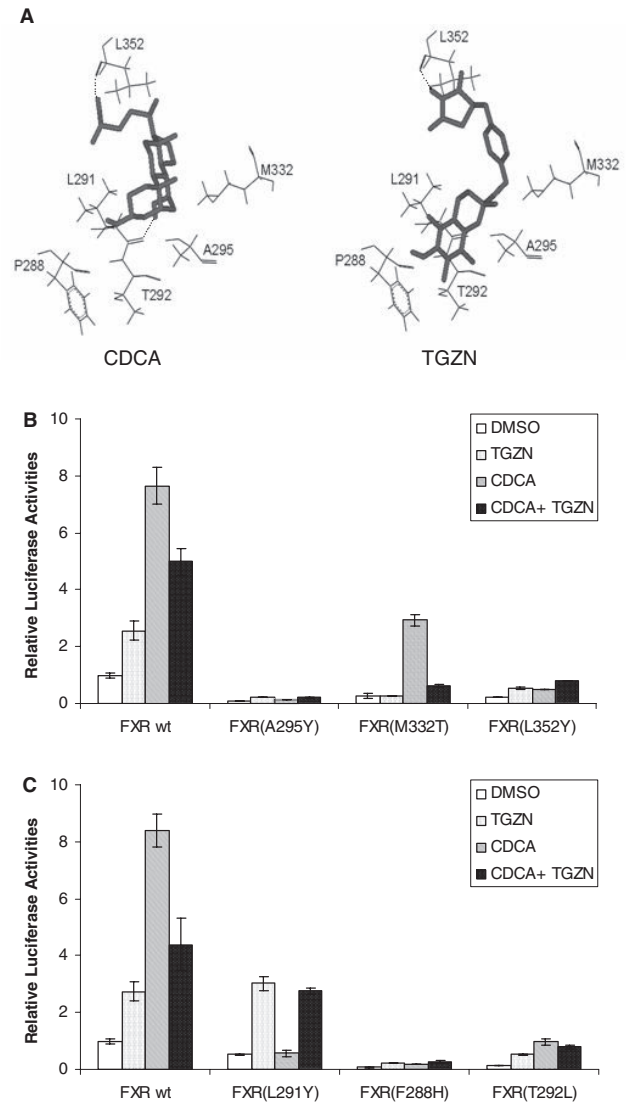

Fig. 6. Functional analyses of docking-guided FXR mutants. In total, six amino acid residues in the FXR LBD predicted to participate in the interaction with troglitazone and/or CDCA were selected for the analysis. Mutagenesis was performed using QuikChange site-directed mutagenesis kit (Stratagene) and FXR wt as template. A, six residues selected for mutational analysis are highlighted in the context of troglitazone (TGZN)- or CDCA-FXR LBD complex. Residues Ala295, Met332, and Leu352 were predicted to interact with both troglitazone and CDCA. Residue Leu291 was predicted to form a hydrogen bond with CDCA but not troglitazone, whereas residues Phe288 and Thr292 were predicted to interact with troglitazone only. B, Huh-7 cells seeded in 24-well plates were cotransfected with BSEP promoter reporter pBSEP(−2.6kb) (100 ng), null *Renilla* luciferase plasmid (10 ng) as internal control, and either FXR wt or a mutant [FXR(A295Y), FXR(M332T), or FXR(L352Y)] (100 ng). Sixteen hours after transfection, cells were treated with vehicle DMSO (0.1%), TGZN (10 μM), CDCA (10 μM), or a combination of both for 30 h. Luciferase activity was assayed with a Dual-Luciferase Reporter Assay System. The data are presented as mean ± S.D. of at least three separate experiments. C, Huh-7 cells seeded in 24-well plates were cotransfected with pBSEP(−2.6kb) (100 ng), null *Renilla* luciferase plasmid (10 ng), and either FXR wt or a mutant [FXR(F288H), FXR(L291Y), or FXR(T292L)] (100 ng), followed by treatment of transfected cells and detection of luciferase activity as described in B.

the side chains of rosiglitazone and pioglitazone were not able to form such interaction mainly due to their smaller sizes and varying structures. The predicted interaction between the α-tocopherol side chain and FXR LBD was validated by functional analysis of docking-guided FXR mutants. Mutation of FXR residues involved in interaction with the α-tocopherol side chain of troglitazone, including Phe288, Thr292, and Ala295, abolished the ability of FXR mutants to respond to troglitazone (Fig. 6), indicating that the interactions between FXR and the side chain play critical roles in the binding of troglitazone to FXR.

CDCA is the most potent endogenous agonist for human FXR, and attempts to crystallize CDCA-bound human FXR LBD failed (Downes et al., 2003). However, a model predicting the interaction between CDCA and human FXR LBD has been reported based on the crystal structure of fexaramine-bound human FXR LBD (Downes et al., 2003). Our modeling of CDCA to FXR LBD is overall consistent with that model. Both models predict identical or similar sets of residues involved in interaction with CDCA. Those residues include Leu291, Ala295, Met332, Ile361, Tyr365, Met454, and Trp473. However, the possible hydrogen bonding between CDCA and FXR LBD varies. Tyr365, Tyr373, and His451 were predicted to potentially form hydrogen bond with CDCA in that study, whereas Leu291 and Leu352 could potentially form hydrogen bond with CDCA based on the current study. Such discrepancy may represent the difference or limitation of the docking programs used for the studies. Compared with CDCA, troglitazone has a relatively larger volume with extended body length (Fig. 5A) as it is the case for fexaramine. Fexaramine has much higher potency in activating FXR than CDCA. It has been proposed that the larger volume of fexaramine makes it more effective in filling in the ligand binding cavity than CDCA (Downes et al., 2003). Consistent with such notion is that troglitazone was predicted to form more stable complex with FXR LBD than CDCA, with binding energy of −10.8 kcal/mol for troglitazone verse −9.4 kcal/mol for CDCA (Fig. 4B). However, such predicted stronger binding was not translated into more potent agonistic activity of troglitazone over CDCA. In fact, troglitazone had approximately 20% of agonistic activity of CDCA (Figs. 1 and 2). It is more significant that troglitazone exhibited potent antagonistic activity, decreasing CDCA-mediated FXR activation by approximately 50% (Figs. 1 and 3). Thus, it is reasonably speculated that, as an FXR modulator, troglitazone could function as a partial agonist in tissues in which endogenous bile acid levels are low, such as breast and prostate, but it could act as a potent antagonist in organs in which a high level of bile acids is present, such as liver and intestine.

In summary, we demonstrated that troglitazone, but not rosiglitazone or pioglitazone, was an FXR modulator and acted as potent antagonist to bile acid-mediated FXR activation. Such troglitazone-specific, PPARγ-independent modulation of FXR signaling pathway may represent one of the mechanisms for the unique activities and toxicity associated with troglitazone.

Acknowledgments

We thank Drs. David Mangelsdorf, Peter Edwards, Matthew Stoner, and Te-Jin Chow for providing human FXR expression plasmid, pTK-2x(phospholipid transfer protein), pPPRE-tk-Luc, and PPARγ construct, respectively. Technical support from the Core Facility of the College of Pharmacy is greatly appreciated.

References

Akiyama TE, Sakai S, Lambert G, Nicol CJ, Matsusue K, Pimprale S, Lee YH, Ricote M, Glass CK, Brewer HB Jr, et al. (2002) Conditional disruption of the peroxisome proliferator-activated receptor gamma gene in mice results in lowered expression

of ABCA1, ABCG1, and apoE in macrophages and reduced cholesterol efflux. *Mol Cell Biol* **22:**2607–2619.
Ananthanarayanan M, Balasubramanian N, Makishima M, Mangelsdorf DJ, and Suchy FJ (2001) Human bile salt export pump promoter is transactivated by the farnesoid X receptor/bile acid receptor. *J Biol Chem* **276:**28857–28865.
Bae MA, Rhee H, and Song BJ (2003) Troglitazone but not rosiglitazone induces G1 cell cycle arrest and apoptosis in human and rat hepatoma cell lines. *Toxicol Lett* **139:**67–75.
Bishop-Bailey D, Walsh DT, and Warner TD (2004) Expression and activation of the farnesoid X receptor in the vasculature. *Proc Natl Acad Sci U S A* **101:**3668–3673.
Blanquicett C, Roman J, and Hart CM (2008) Thiazolidinediones as anti-cancer agents. *Cancer Ther* **6:**25–34.
Camp HS, Li O, Wise SC, Hong YH, Frankowski CL, Shen X, Vanbogelen R, and Leff T (2000) Differential activation of peroxisome proliferator-activated receptor-gamma by troglitazone and rosiglitazone. *Diabetes* **49:**539–547.
Chaffer CL, Thomas DM, Thompson EW, and Williams ED (2006) PPARgamma-independent induction of growth arrest and apoptosis in prostate and bladder carcinoma. *BMC Cancer* **6:**53.
Davies GF, Khandelwal RL, Wu L, Juurlink BH, and Roesler WJ (2001) Inhibition of phosphoenolpyruvate carboxykinase (PEPCK) gene expression by troglitazone: a peroxisome proliferator-activated receptor-gamma (PPARgamma)-independent, antioxidant-related mechanism. *Biochem Pharmacol* **62:**1071–1079.
Davies GF, McFie PJ, Khandelwal RL, and Roesler WJ (2002) Unique ability of troglitazone to up-regulate peroxisome proliferator-activated receptor-gamma expression in hepatocytes. *J Pharmacol Exp Ther* **300:**72–77.
Deng R, Yang D, Radke A, Yang J, and Yan B (2007) Hypolipidemic agent guggulsterone regulates the expression of human bile salt export pump: dominance of transactivation over FXR-mediated antagonism. *J Pharmacol Exp Ther* **320:**1153–1162.
Deng R, Yang D, Yang J, and Yan B (2006) Oxysterol 22(R)-hydroxycholesterol induces the expression of the bile salt export pump through nuclear receptor farnesoid X receptor but not liver X receptor. *J Pharmacol Exp Ther* **317:**317–325.
Downes M, Verdecia MA, Roecker AJ, Hughes R, Hogenesch JB, Kast-Woelbern HR, Bowman ME, Ferrer JL, Anisfeld AM, Edwards PA, et al. (2003) A chemical, genetic, and structural analysis of the nuclear bile acid receptor FXR. *Mol Cell* **11:**1079–1092.
Goodwin B, Jones SA, Price RR, Watson MA, McKee DD, Moore LB, Galardi C, Wilson JG, Lewis MC, Roth ME, et al. (2000) A regulatory cascade of the nuclear receptors FXR, SHP-1, and LRH-1 represses bile acid biosynthesis. *Mol Cell* **6:**517–526.
Hilding A, Hall K, Skogsberg J, Ehrenborg E, and Lewitt MS (2003) Troglitazone stimulates IGF-binding protein-1 by a PPAR gamma-independent mechanism. *Biochem Biophys Res Commun* **303:**693–699.
Huang W, Ma K, Zhang J, Qatanani M, Cuvillier J, Liu J, Dong B, Huang X, and Moore DD (2006) Nuclear receptor-dependent bile acid signaling is required for normal liver regeneration. *Science* **312:**233–236.
Journe F, Laurent G, Chaboteaux C, Nonclercq D, Durbecq V, Larsimont D, and Body JJ (2008) Farnesol, a mevalonate pathway intermediate, stimulates MCF-7 breast cancer cell growth through farnesoid-X-receptor-mediated estrogen receptor activation. *Breast Cancer Res Treat* **107:**49–61.
Kaeding J, Bouchaert E, Bélanger J, Caron P, Chouinard S, Verreault M, Larouche O, Pelletier G, Staels B, Bélanger A, et al. (2008) Activators of the farnesoid X receptor negatively regulate androgen glucuronidation in human prostate cancer LNCAP cells. *Biochem J* **410:**245–253.
Lebovitz HE (2002) Differentiating members of the thiazolidinedione class: a focus on safety. *Diabetes Metab Res Rev* **18 (Suppl 2):**S23–S29.
Lecomte J, Flament S, Salamone S, Boisbrun M, Mazerbourg S, Chapleur Y, and Grillier-Vuissoz I (2008) Disruption of ERalpha signalling pathway by PPAR-gamma agonists: evidences of PPARgamma-independent events in two hormone-dependent breast cancer cell lines. *Breast Cancer Res Treat* **112:**437–451.
Liu Y, Binz J, Numerick MJ, Dennis S, Luo G, Desai B, MacKenzie KI, Mansfield TA, Kliewer SA, Goodwin B, et al. (2003) Hepatoprotection by the farnesoid X receptor agonist GW4064 in rat models of intra- and extrahepatic cholestasis. *J Clin Invest* **112:**1678–1687.
Marcy TR, Britton ML, and Blevins SM (2004) Second-generation thiazolidinediones and hepatotoxicity. *Ann Pharmacother* **38:**1419–1423.
Ming M, Yu JP, Meng XZ, Zhou YH, Yu HG, and Luo HS (2006) Effect of ligand troglitazone on peroxisome proliferator-activated receptor gamma expression and cellular growth in human colon cancer cells. *World J Gastroenterol* **12:**7263–7270.
Modica S, Murzilli S, Salvatore L, Schmidt DR, and Moschetta A (2008) Nuclear bile acid receptor FXR protects against intestinal tumorigenesis. *Cancer Res* **68:**9589–9594.
Morris GM, Goodsell DS, Halliday RS, Huey R, Hart WE, Belew RK, and Olson AJ (1998) Automated docking using a lamarckian genetic algorithm and empirical binding free energy function. *J Comput Chem* **19:**1639–1662.
Nolte RT, Wisely GB, Westin S, Cobb JE, Lambert MH, Kurokawa R, Rosenfeld MG, Willson TM, Glass CK, and Milburn MV (1998) Ligand binding and co-activator assembly of the peroxisome proliferator-activated receptor-gamma. *Nature* **395:**137–143.
Ogino M, Nagata K, and Yamazoe Y (2002) Selective suppressions of human CYP3A forms, CYP3A5 and CYP3A7, by troglitazone in HepG2 cells. *Drug Metab Pharmacokinet* **17:**42–46.
Park YJ, Qatanani M, Chua SS, LaRey JL, Johnson SA, Watanabe M, Moore DD, and Lee YK (2008) Loss of orphan receptor small heterodimer partner sensitizes mice to liver injury from obstructive cholestasis. *Hepatology* **47:**1578–1586.
Rizos CV, Liberopoulos EN, Mikhailidis DP, and Elisaf MS (2008) Pleiotropic effects of thiazolidinediones. *Expert Opin Pharmacother* **9:**1087–1108.
Sinal CJ, Tohkin M, Miyata M, Ward JM, Lambert G, and Gonzalez FJ (2000) Targeted disruption of the nuclear receptor FXR/BAR impairs bile acid and lipid homeostasis. *Cell* **102:**731–744.
Song X, Kaimal R, Yan B, and Deng R (2008) Liver receptor homolog 1 transcriptionally regulates human bile salt export pump expression. *J Lipid Res* **49:**973–984.
Stoner MA, Auerbach SS, Zamule SM, Strom SC, and Omiecinski CJ (2007) Transactivation of a DR-1 PPRE by a human constitutive androstane receptor variant expressed from internal protein translation start sites. *Nucleic Acids Res* **35:**2177–2190.
Swales KE, Korbonits M, Carpenter R, Walsh DT, Warner TD, and Bishop-Bailey D (2006) The farnesoid X receptor is expressed in breast cancer and regulates apoptosis and aromatase expression. *Cancer Res* **66:**10120–10126.
Van Mil SW, Milona A, Dixon PH, Mullenbach R, Geenes VL, Chambers J, Shevchuk V, Moore GE, Lammert F, Glantz AG, et al. (2007) Functional variants of the central bile acid sensor FXR identified in intrahepatic cholestasis of pregnancy. *Gastroenterology* **133:**507–516.
Walker AB, Naderali EK, Chattington PD, Buckingham RE, and Williams G (1998) Differential vasoactive effects of the insulin sensitizers rosiglitazone (BRL 49653) and troglitazone on human small arteries in vitro. *Diabetes* **47:**810–814.
Wang L, Soroka CJ, and Boyer JL (2002) The role of bile salt export pump mutations in progressive familial intrahepatic cholestasis type II. *J Clin Invest* **110:**965–972.
Wang R, Salem M, Yousef IM, Tuchweber B, Lam P, Childs SJ, Helgason CD, Ackerley C, Phillips MJ, and Ling V (2001) Targeted inactivation of sister of P-glycoprotein gene (spgp) in mice results in nonprogressive but persistent intrahepatic cholestasis. *Proc Natl Acad Sci U S A* **98:**2011–2016.
Wang YD, Chen WD, Moore DD, and Huang W (2008) FXR: a metabolic regulator and cell protector. *Cell Res* **18:**1087–1095.
Willson TM, Cobb JE, Cowan DJ, Wiethe RW, Correa ID, Prakash SR, Beck KD, Moore LB, Kliewer SA, and Lehmann JM (1996) The structure-activity relationship between peroxisome proliferator-activated receptor gamma agonism and the antihyperglycemic activity of thiazolidinediones. *J Med Chem* **39:**665–668.
Yang F, Huang X, Yi T, Yen Y, Moore DD, and Huang W (2007) Spontaneous development of liver tumors in the absence of the bile acid receptor farnesoid X receptor. *Cancer Res* **67:**863–867.
Yu J, Lo JL, Huang L, Zhao A, Metzger E, Adams A, Meinke PT, Wright SD, and Cui J (2002) Lithocholic acid decreases expression of bile salt export pump through farnesoid X receptor antagonist activity. *J Biol Chem* **277:**31441–31447.
Zhao A, Yu J, Lew JL, Huang L, Wright SD, and Cui J (2004) Polyunsaturated fatty acids are FXR ligands and differentially regulate expression of FXR targets. *DNA Cell Biol* **23:**519–526.

Address correspondence to: Dr. Ruitang Deng, Department of Biomedical and Pharmaceutical Sciences, Center for Pharmacogenomics and Molecular Therapy, College of Pharmacy, University of Rhode Island, 41 Lower College Rd., Kingston, RI 02881. E-mail: engr@mail.uri.edu.